Current Research in Food Science 10 (2025) 101046

Contents lists available at ScienceDirect

Current Research in Food Science

journal homepage: www.sciencedirect.com/journal/current-research-in-food-science

Preparation, structural characterization, and functional properties of a tilapia-soybean dual proteins: Effects of different complexation modes

Xinyi Qin, Pengzhi Hong, Liangyu Zhao, Mengya Xie, Chunxia Zhou *, Qingguan Liu **

College of Food Science and Technology, Guangdong Ocean University, Guangdong Provincial Key Laboratory of Aquatic Product Processing and Safety, Guangdong Provincial Engineering Technology Research Center of Marine Food, Guangdong Provincial Modern Agricultural Science and Technology Innovation Center, Zhanjiang, 524088, China

ARTICLE INFO

Handling editor: Dr. Xing Chen

Keywords:
Tilapia protein isolate
Soybean protein isolate
Dual protein
pH-regulation
Functional properties

ABSTRACT

The limited functional properties of tilapia protein isolate (TPI), such as low solubility, emulsification, and foaming, restrict its use in the food industry. However, combining it with hydrophilic proteins can improve these properties. Different assembly methods may affect the structure and functionality of the resulting dual proteins. To study this, tilapia-soybean protein mixtures (T-SPM), complexes (T-SPC), and co-precipitates (T-SPCP) were prepared using physical mixing, pH-regulated complexation, and pH-regulated co-precipitation. The effects of these methods on the structure and functional properties of the tilapia-soybean dual proteins were then analyzed. Structural analysis revealed that TPI combined with SPI through non-covalent forces and disulfide bonds under pH-regulation, leading to structural changes. Compared to T-SPCP, T-SPC showed more hydrophilic groups, with increased free sulfhydryl groups, disulfide bonds, α-helices, and zeta potential, alongside reduced surface hydrophobicity and smaller flake structures. Functional analysis indicated that pH-regulated assembly methods significantly improved the properties of the dual proteins compared to T-SPM. T-SPC exhibited higher solubility, emulsification, and foaming capacity than T-SPCP, which had a more aggregated structure due to pH adjustment to 4.5 during co-precipitation, contributing to its better thermal stability. Thus, T-SPC, assembled by pH-regulation from 12.0 to 7.0, demonstrated superior characteristics. This study offers a theoretical foundation for developing functional dual proteins and their food industry applications.

1. Introduction

Protein is an essential nutrient for both humans and animals, with a significant global demand for protein products each year. In China, the export value of protein substances increased from $3227.69 million in 2019 to $4866 million in 2022 (National date, 2024). Compared to plant and animal proteins, complex proteins hold greater research and utilization value. Due to the increasing demand for environmentally sustainable development, there is growing interest in mixing plant and animal proteins to create products with superior nutritional and textural properties (Alves and Tavares, 2019; Jafarzadeh et al., 2024). Mixed proteins can combine the nutritional and health benefits of different sources of protein raw materials to replace traditional plant and animal proteins in the human diet. Mixed proteins also explores quantitative relationships and unique molecular effects of proteins from various sources (Yin Zonglun Wang, 2007), thereby maximizing protein value.

Tilapia is a freshwater fish widely farmed in Africa and Asia. This species has attracted wide attention because of its low fat level, high protein content, and rich unsaturated fatty acids, it is especially suitable for children and the elderly (Shaheen et al., 2016). Along with various high-quality sources of animal and plant protein, tilapia has a low cost, high protein nutritional value, and is easy to obtain. Therefore, tilapia is expected to become an important source of animal protein in the future (Ali Mekouar, 2019). Moreover, the content of tilapia protein isolate (TPI) in the tilapia body is approximately 18 %. It comprises rich and complete proteins with an amino acid composition similar to human tissue, thus possessing high physiological value (Yin Zonglun Wang, 2007). However, fish proteins exhibit low solubility (<10 %, w/v) in water within the pH range of 4–7 (Mohan et al., 2006). Processing alters protein structures, leading to poor thermal stability and solubility too. Consequently, the commercial applications of TPI are significantly limited (Li et al., 2024). Some studies suggest that protein-protein

* Corresponding author. College of Food Science and Technology, Guangdong Ocean University, Zhanjiang, 524088, China.
** Corresponding author.
E-mail addresses: chunxia.zhou@163.com (C. Zhou), liuqingguansdk@163.com (Q. Liu).

https://doi.org/10.1016/j.crfs.2025.101046
Received 2 December 2024; Received in revised form 7 March 2025; Accepted 1 April 2025
Available online 1 April 2025

interactions can enhance the functional properties of proteins, including solubility (Lin et al., 2017). The solubility, stability, and emulsification properties of proteins are crucial considerations in food processing and manufacturing (Wang et al., 2020a). Additionally, complex with nutritionally balanced proteins is an effective method to improve protein nutritional value. Thus, selecting alternative protein sources and techniques to explore the mechanisms underlying structural interactions between different proteins is essential. Soybean protein isolate (SPI), primarily composed of 7S/11S globulin (70 %), is known for its high nutritional quality and ideal processing characteristics (Tian et al., 2018). By the way, the first limiting amino acid of TPI is lysine, while the limiting amino acid of SPI is methionine. The addition of soy protein isolate (SPI) to tilapia protein isolate (TPI) in a variety of complex ways can not only combine the nutritional advantages of the two but also improve their functional properties and stability. This method effectively makes up for the deficiencies of a single protein in terms of function and nutrition, so that the co-assembled protein has the amino acid composition of both (Wang et al., 2021).

There are some ways to recombine proteins, studies have been conducted to create novel protein complexes with co-constructed internal structures by co-solubilizing rice and pea proteins at pH 12.0, indicating that the unfolding of both protein molecules through their secondary structures at this pH is driven by hydrophobic forces (Wang et al., 2020b). The partial substitution of plant protein for animal protein to develop new products is of great concern. Cheng et al. (2024) prepared a heat-induced complex milk protein gel with a final total protein concentration of 10 % (w/w) using a mixture of whey protein isolate (WPI) and SPI. Kristensen et al. (2022) investigated the interactions of two proteins containing free thiols, β-lactoglobulin, and leguminous proteins, highlighting the importance of disulfide, hydrophobic, and electrostatic interactions. Hydrating rice and cod proteins at pH 12.0 and subsequently re-neutralizing them resulted in the preparation of extremely water-soluble nanoscale hydrophilic colloidal co-assemblies of rice and cod proteins (Wang et al., 2021). Zhao et al. (2024) examined the alterations induced by three modifications (pH shifting, sonication, and combined pH transfer sonication) of pure whey protein, pea protein, and mixed whey-pea protein to explore the properties of the mixed system of animal and plant proteins. Furthermore, tilapia-soybean protein co-precipitates (TSPCs) were created using various mass ratios of tilapia fish and soybean meal. Proteomic analysis indicated that, compared to isolate protein, TSPCs demonstrated stronger biological characteristics and the ability to engage in a broader range of biochemical metabolism and signaling pathways (Liu et al., 2024).

Based on the above findings, multiple assembly methods (pH regulation, ultrasonic treatment, pH regulation combined with ultrasonic treatment, and high-pressure pulse) have been used to combine two proteins and enhance their functional properties and nutritional value. However, the effects of different methods on the structural and functional properties of tilapia-soybean proteins may vary and have not been thoroughly studied and compared. Understanding how dual protein processing affects protein structure and functional properties characterization is crucial for efficiently developing high-performance dual proteins. Therefore, in this study, the tilapia-soybean dual proteins were constructed using physical mixing, pH-regulated complexation, and co-precipitation, and the effects of different preparation processes on the structure and functional properties characterization of the dual proteins were studied. This study aims to identify the most efficient pathways for the formation of dual proteins, and provide a basis for their subsequent application in the development of novel protein foods.

2. Materials and methods

2.1. Materials

Low-temperature defatted soybean meal (YP5084C) was purchased from Yuwang Ecological Food Industry Co. Ltd (Dezhou, Shandong), with a protein content of 55.0 %. Live tilapia from the local aquatic market (Zhanjiang, China) were transported to the laboratory on ice. To reduce the pain, the fish was frozen into a coma, and then it was hit to death with a stick to collect the back muscles at room temperature. The molecular weight of the dialysis bag is 8000–14000 Da. Prestained color protein ladder contains 10 purified pre-dyed proteins ranging from 6.5 to 270 kDa, and the size of the standard strip of molecular weight of the predicted protein is obtained according to the size comparison of the molecular weight of the non-predyed protein. SDS-PAGE rapid electrophoresis gels, and 8-Aniline-1-naphthalenesulfonic acid (ANS) fluorescent probe were purchased from Shanghai Biyuntian Biotechnology Co. Ltd (Shanghai, China). The Lowry assay kit was purchased from Shanghai Lida Biotechnology Co., LTD. (Shanghai, China). Powdered ethylenediamine tetraacetic acid (EDTA), 5,5' -dithiobis - (2-nitrobenzoic acid) (DTNB), and all other reagents are analytical grades.

2.2. Protein extraction and preparation of complex dual proteins

2.2.1. Extraction of TPI and SPI

The preparation of TPI and SPI was based on the method of Liu (Liu et al., 2024) with minor modifications. TPI and SPI were extracted and prepared by alkali-soluble acid precipitation. The specific process was shown in Fig. 1.

2.2.2. Preparation of tilapia-soybean complex dual proteins

According to the method described by Li and Liu (Li et al., 2024; Liu et al., 2024) with slight modifications, tilapia-soybean protein mixtures (T-SPM), tilapia-soybean protein complexes (T-SPC), and tilapia-soybean protein co-precipitates (T-SPCP) were prepared from TPI and SPI by physical mixing, pH-regulated complexation and pH-regulated co-precipitation, respectively. The specific process was shown in the flow chart in Fig. 2, and the preparation of T-SPM, T-SPC and T-SPCP was carried out according to red, black and blue paths respectively.

2.3. Structure characterization of complex dual proteins

The freeze-dried protein samples (2 g) were dispersed in 100 mL deionized water, and stirred for 2 h at room temperature. After centrifuging (1500×*g*, 4 °C, 15 min) with Avanti J-26S XP (Beckman Coulter, USA), the protein supernatant was collected for electrophoresis, surface hydrophobicity, zeta potential and spectra detection, and the protein content was determined by Lowry method. The protein supernatant was stored at 4 °C and detection process was completed in 24 h.

2.3.1. Sodium dodecyl sulphate polyacrylamide gel electrophoresis (SDS-PAGE)

SDS-PAGE was performed based on Liu and Xiong (2000). The protein supernatant (2 mg/mL) was mixed with sample buffer (1:4, v/v) and heated at 100 °C for 5 min with thermostatic water bath (Aohua Instrument Co., LTD., Jiangsu, China). The heated mixtures (10 μL) were loaded onto 12 % separation gels and 5 % stacking gels. Electrophoresis was performed for 60 min at 120 V using an electrophoresis power supply (DYY-7C). The gels were stained with Coomassie blue R250 and destained with a solution (ethanol: glacial acetic acid: water = 150 mL: 50 mL: 300 mL). Finally, the protein bands were visualized using the Bio-Rad chemical gel imaging system (Bio-Rad, Hercules, USA).

2.3.2. Surface hydrophobicity (H_0) and zeta potential

H_0 was determined using the ANS fluorescent probe method (Jianhua Liu et al., 2019). The protein supernatant was diluted with 10 mM phosphate-buffered saline (PBS, pH 7.0) into five concentration gradients (0.15–0.015 mg/mL). Then, 10 μL of 8 mM ANS was added to 4 mL of each sample and incubated in the dark for 15 min. The fluorescence intensity was measured at the excitation wavelength of 390 nm and the emission wavelength of 484 nm using fluorescence spectrometer

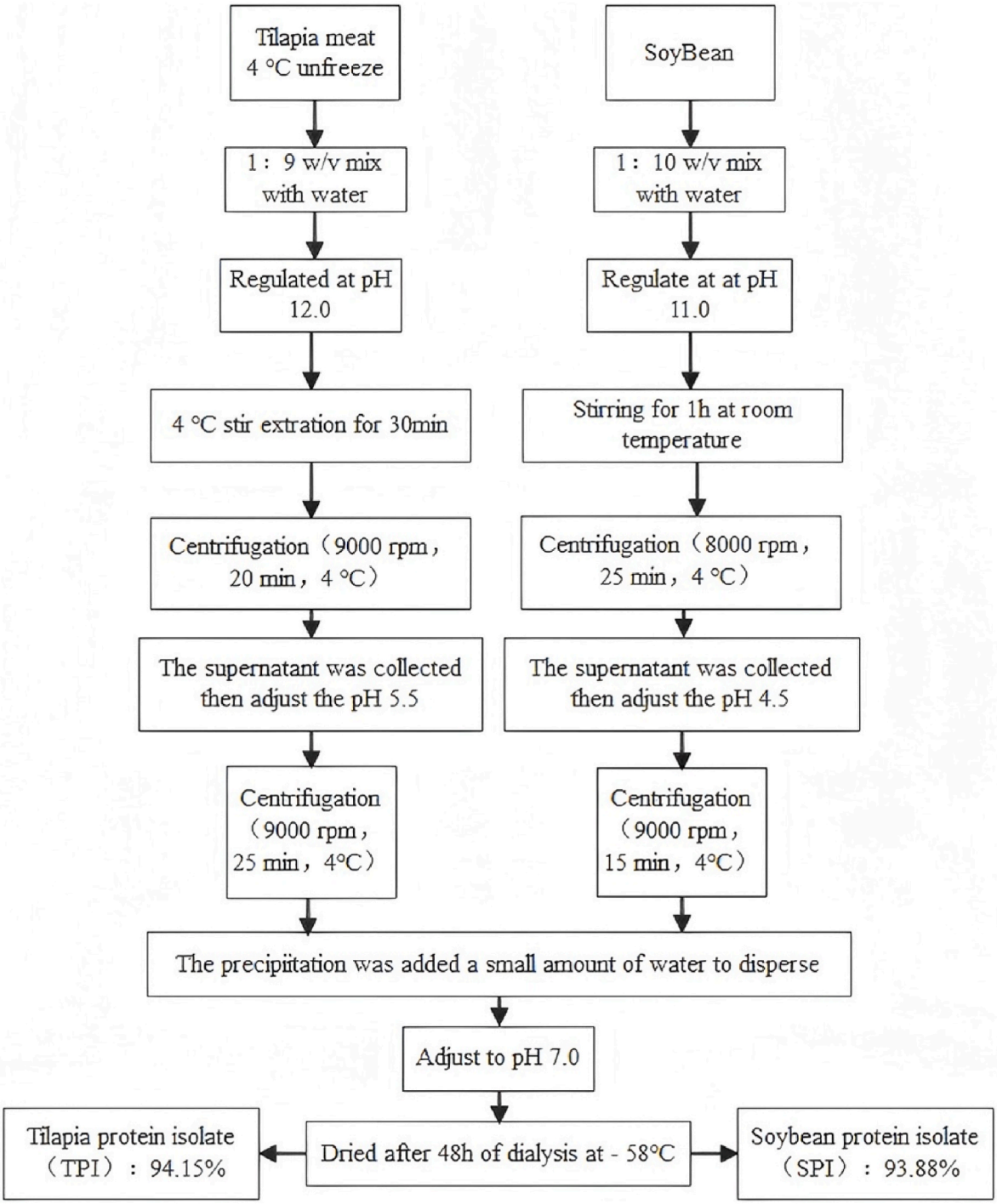

Fig. 1. Flow chart for the preparation of TPI and SPI.

(G9800A, Agilent, USA). The H_0 of the protein (representing the initial slope of fluorescence versus and protein concentration) was calculated by linear regression.

The protein was diluted to 1 mg/mL with PBS, and the zeta potential was determined using a nanoparticle surface potential tester (Holtsville, NY, USA).

2.3.3. Total sulfhydryl (SH_T) and active sulfhydryl (SH_A) contents

The SH_T and SH_A contents were determined by the Ellman method (Han et al., 2019). To determine the SH_T content, 0.1 g of protein was mixed with 10 mL of 0.2 M PBS (pH 8.0, containing 86 mM Tris, 90 mM glycine, 4 mM EDTA, and 8 M urea) and centrifuged for 10 min at 10, 000×*g* at 4 °C. The supernatant was collected, and 1 mL was added to 4 mL of 0.2 M Tris-Gly buffer and 0.1 mL of 10 mM DTNB. The absorbance was measured using a UV–visible spectrophotometer (GBC Scientific Equipment Pty Ltd Braeside, Victoria, Australia) at a wavelength of 412 nm. To evaluate the content of SH_A and S-S bonds, the supernatant (1 mL) was mixed with 4 mL of 0.2 M Tris-Gly buffer and 0.1 mL of *β*-mercaptoethanol. The mixture was stirred at 25 °C for 1 h, and then 10 mL of 12 % (w/v) trichloroacetic acid (TCA) solution was added. After standing for 1 h, the mixture was precipitated twice with 5 mL of TCA solution. The final precipitate was dissolved in 10 mL of 0.2 M Tris-Gly buffer, and 0.1 mL of 10 mM DTNB was added. After 20 min, the absorbance was measured at 412 nm. This process was repeated three

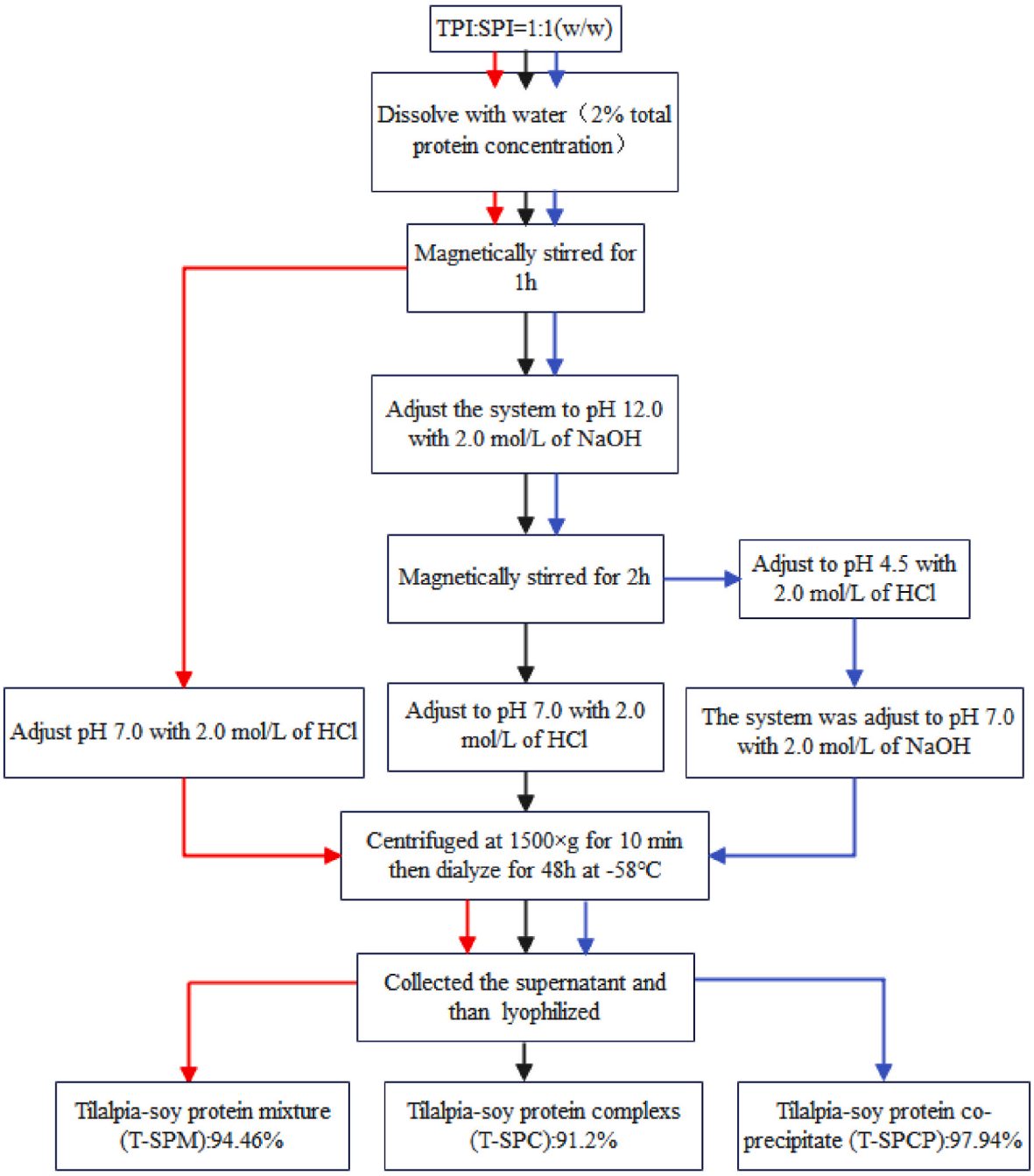

Fig. 2. Flow chart for the preparation of tilapia-soybean complex dual proteins. *Note:* The produced protein is vacuum-packed and stored at 4 °C in the refrigerator.

times for each sample. The contents of SH_T and SH_A were calculated using the following equations:

$$SH\ (\text{mol/g}) = 73.53 \times A_{412} \times D/\text{C} \quad (1)$$

$$S-S(mol/g) = \frac{SH_T - SH_A}{2} \quad (2)$$

where, A_{412} is the absorbance at 412 nm, D is the dilution factor (5 and 10 for SH_A and SH_T, respectively), and C is the protein concentration (mg/mL).

2.3.4. Intrinsic emission fluorescence spectra

The protein supernatant was diluted to 0.02 mg/mL with 10 mM PBS. Intrinsic emission fluorescence spectra of the protein samples were obtained using an RF-5301 PC spectrofluorophotometer (Shimadzu Corp., Kyoto, Japan). The protein solutions were excited at 280 nm, and emission spectra were recorded from 300 to 460 nm with a constant slit width of 5 nm for both excitation and emission (Liu et al., 2012).

2.3.5. Ultraviolet (UV) spectra

UV spectral scanning was conducted according to the method described by Liu et al. (2012), with slight modifications. The protein supernatant was diluted to 0.02 mg/mL using 10 mM PBS. The UV scan was performed over a wavelength range of 190–400 nm, at a scanning rate of 100 nm/min and a resolution of 0.2 nm, using a UV–visible spectrophotometer.

2.3.6. Fourier transform infrared (FTIR) spectroscopy

FTIR spectroscopy was performed following the method proposed by Huang et al. (Guo Huang et al., 2023). The freeze-dried protein powder

was mixed with KBr powder at a ratio of 1:100 (w/w), and then the mixture was pressed into pellets. The thin slices were scanned in the wavenumber range of 4000-400 cm^{-1} with a resolution of 4 cm^{-1} and 32 scans. After baseline correction and smoothing, the FTIR spectra of the protein samples were recorded using an 8400S spectrometer (Shimadzu Corporation, Kyoto, Japan).

2.3.7. Circular dichroism (CD) spectroscopy

Far-UV (180–260 nm) CD of proteins was determined using a previously described method with some modifications (Wang et al., 2018) The protein supernatant was diluted to 0.2 mg/mL with 10 mM PBS. CD measurements were made using a 10 mm path length quartz cell by Chirascan V100 Circular Dichroic Spectrum (Applied Photophysics Ltd, Leatherhead, Surrey, UK). The 10 mM PBS without protein samples was used as a control. Data were expressed as molar ellipticity, and the CD spectral data were plotted using Origin software (OriginLab, Northampton, MA, USA).

2.3.8. Scanning electron microscope (SEM) observation

A small amount of the freeze-dried protein powder was placed on a metal stub and coated with a layer of gold nanoparticles (10 nm thick). Electron micrographs were obtained using an SEM (JSM-7610-F, JEOL, Japan) under vacuum conditions. All SEM images were obtained at 1000 × magnification.

2.4. Functional properties characterization of complex dual proteins

2.4.1. Solubility

The method for determining protein solubility was adapted from Britten (Britten et al., 1994). Protein powders were suspended at a concentration of 10 mg/mL in deionized water, and the pH was adjusted to 7.0 using either 1.0 M HCl or 1.0 M NaOH. The mixtures were gently stirred for 2 h at 25 °C and then centrifuged at 10,000×*g* for 20 min. The protein content of the supernatant was determined using the Lowry method. Solubility (%) was calculated as the ratio of soluble protein in the supernatant after centrifugation to the total protein in the dispersion before centrifugation.

2.4.2. Emulsifying activity index (EAI) and emulsifying stability index (ESI)

The EAI and ESI of protein samples were determined using the turbidity method (Agyare et al., 2009). A 1 % protein dispersion and soybean oil were mixed in a 3:1 (w/w) ratio. The mixture was homogenized at high speed (12,000 rpm) for 2 min using a shear homogenizer (ULTRA-TURRAX T18, IKA, Germany) to form a uniform emulsion. Initially, 50 μL of emulsion was collected from the bottom and added to 5 mL of a 0.1 % SDS solution. This mixture was then agitated using a vortex mixer (Chirember Instrument Manufacturing Co., Ltd., Jiangsu, China). After 30 min, an additional 50 μL was taken from the bottom of the emulsion and again added to 5 mL of the 0.1 % SDS solution, followed by mixing. The absorbance of the solution was measured at a wavelength of 500 nm. The formulas used for calculating EAI and ESI are as follows:

$$\mathrm{EAI}\left(\mathrm{m}^2/\mathrm{g}\right)=\frac{2\times 2.303\times A_0\times D}{C\times \varnothing\times L\times 10^4} \tag{3}$$

$$\mathrm{ESI}(\mathrm{min})=\frac{A_0}{A_0-A_{30}}\times \Delta t \tag{4}$$

where A_0 was the initial absorbance of the sample, A_{30} was the absorbance of the sample mixed with SDS after 30 min, D was the dilution ratio (100), Φ was the oil phase volume fraction (0.25), L was the optical path length (1 cm), C was the concentration of protein solution (0.01 g/mL), $\triangle t = 30$ min.

2.4.3. Foaming capacity (FC) and foam stability (FS)

FC and FS were analyzed following the method of Tian et al. (2022) with slight adjustments. A 40 mL protein suspension (10 mg/mL) was sheared at 12,000 rpm for 2 min using a high-shear dispersion homogenizer (JRJ300-S, Shanghai Sample Model Factory, Shanghai, China) to form foam. The foams were immediately transferred into a 100 mL graduated cylinder, and FC was calculated by comparing the volume of the foam with the volume of the initial solution. FS was determined by measuring the volume of the foam layer before and after standing at 25 °C for 30 min. The foaming volumes at 0 min and 30 min were recorded. FC and FS values were calculated as follows:

$$\mathrm{FC}(\%)=\frac{V_1-V_0}{V_0}\times 100 \tag{5}$$

$$\mathrm{FS}(\%)=\frac{V_0-V_2}{V_0}\times 100 \tag{6}$$

where V_0 is the volume of the protein suspension (40 mL), V_1 is the volume of foam immediately after shearing, and V_2 is the volume of foam 30 min after shearing.

2.4.4. Thermal stability

The thermal denaturation temperature of protein samples was determined using a simultaneous thermal analyzer (STA449F3, NETZSCH, Bavaria, Germany). The protein samples (9.0 mg) were sealed in aluminum trays and heated from 30 to 150 °C at 10 °C/min (Ricci et al., 2018). Nitrogen was a carrier gas at a flow rate of 50 mL/min. Peak temperature values indicated the thermal denaturation temperature.

2.5. Statistical analysis

All experiments were repeated at least three times. One-way analysis of variance (ANOVA) was performed using IBM SPSS Statistics 27.0 (International Business Machines Corporation, Armonk, NY, USA). Differences between least-squares means were determined using Duncan's multiple-range test. All figures were drawn using Origin 2023. $p < 0.05$ was considered statistically significant, and results were expressed as mean ± standard deviation.

3. Results and discussion

3.1. Structural characterization

3.1.1. SDS-PAGE analysis

As shown in Fig. 3, SPI and TPI exhibited distinct characteristic compositional bands. SPI displayed bands at 71 kDa, 50 kDa, 35 kDa, and 17 kDa, representing the α and β subunits of β-conglycinin and the acidic and basic subunits of glycinin, respectively. TPI showed bands at 200 kDa, 42 kDa, 34 kDa, and 13 kDa, corresponding to myosin heavy chain (MHC), actin (AC), promyosin (TnT), and myosin light chain (MLC), respectively (Pramono et al., 2019). The three dual proteins contained most of the subunit bands from SPI and TPI, as illustrated in Fig. 3, including the α, β, acidic, and basic subunits of SPI, as well as MHC, AC, TnT, and MLC of TPI. This indicated that T-SPC and T-SPCP are composed of both SPI and TPI, corroborating the previous research on the preparation of co-precipitated protein from soybean meal and tilapia (Liu et al., 2024).

3.1.2. H_0 and zeta potential analysis

Appropriate surface hydrophobicity is critical for protein stability, solubility, adsorption behavior, and thermal stability (Yan et al., 2021). As shown in Fig. 4A, the H_0 of T-SPM and T-SPC was between those of SPI and TPI. This finding aligns with the results that the H_0 of TPI and casein complexes lies between the two proteins (Li et al., 2024). The

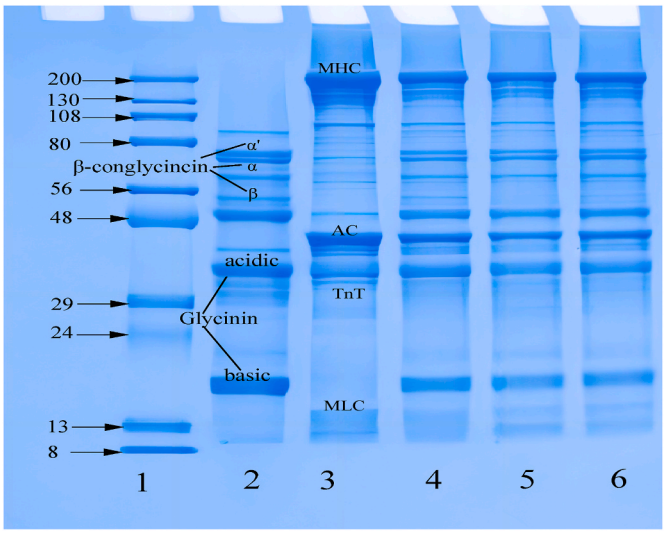

Fig. 3. SDS-PAGE of SPI, TPI, and tilapia-soybean dual proteins. Band 1 represents standard proteins; Band 2 represents SPI; Band 3 represents TPI; Band 4–6 represents T-SPM, T-SPC, and T-SPCP, respectively. MHC is myosin heavy chain; AC is actin; TM α1 is promyosin; TnT is troponin; MLC is myosin light chain.

surface charges of proteins are key determinants of their water solubility (Song et al., 2013). As depicted in Fig. 4B, the zeta potential of T-SPM and T-SPC was also between those of SPI and TPI. A higher absolute potential correlates with lower H_0. Compared to T-SPCP, T-SPC exhibited lower H_0 and higher absolute potential, indicating that T-SPC may have better stability and solubility. However, during co - precipitation, the adjustment of pH to 4.5 led to intermolecular binding and aggregation, which might endow T - SPCP with a dense structure.

3.1.3. -SH and S-S contents

Sulfhydryl groups and disulfide bonds are essential for protein functionality and maintaining tertiary structure. Changes in -SH groups often indicate the degree of protein denaturation (Beveridge et al., 1974). As shown in Fig. 4C, the contents of SH_T and S-S in T-SPC and T-SPCP were lower than those in SPI and TPI, with T-SPM showing minimal change, suggesting that pH-regulating treatment facilitated the interchange of -SH and S-S groups. This may be attributed to the protonation of SH groups, which restricts the formation of S-S bonds. Additionally, cysteine residues may form sulfuric acid groups at pH > 9, making them susceptible to degradation and leading to a decline in S-S bonds (Kheto et al., 2024). Consequently, the contents of -SH and S-S in T-SPC and T-SPCP were lower than those in T-SPM. Furthermore, the decrease in S-S content indicates the unfolding of protein molecules. Alkaline treatment can disrupt protein structures, which exposes polar residues to oxidation and reducing -SH content. The variations in SH_T and S-S contents among the dual proteins suggested that the pH-regulation significantly affects the -SH and S-S levels of proteins (Kheto et al., 2024). Compared to T-SPC, the further co-precipitation at pH 4.5 in T-SPCP resulted in more pronounced changes in molecular structure, leading to increased exposure of SH_T, protein oxidation, and a reduction in -SH content. The generated disulfide bonds may oxidize to form sulfonic acid or other oxidation products (Wang et al., 2016), which may potentially induce the aggregation of proteins and reduce their solubility.

3.1.4. Intrinsic fluorescence spectra analysis

Tryptophan residues are highly sensitive to their polar environment. Thus, the intrinsic fluorescence spectrum of tryptophan serves as a suitable index for detecting protein tertiary conformation (Wang et al., 2023). As shown in Fig. 5A, TPI, SPI, and T-SPM exhibited fluorescence absorption peaks at 313 nm, while T-SPC and T-SPCP displayed no significant fluorescence absorption at this wavelength. The tryptophan fluorescence intensity of T-SPCP and T-SPC was significantly greater than that of TPI and SPI, with a notable redshift to 334 nm, indicating that the changes of tertiary structure of the dual proteins were substantially caused by the change of pH. The pH adjustment to 12.0 resulted in strong electrostatic repulsion and a more open structure, exposing more tryptophan. However, following refolding through isoelectric point precipitation at pH 4.5 and neutral adjustment, it was challenging for T-SPCP to return to its initial structure (Jiang et al., 2009). Therefore, the fluorescence intensity of T-SPCP obtained through pH-regulated co-precipitation was higher than that of T-SPC from pH-regulated complexation, suggesting that the co-precipitation at pH 4.5 and refolding may have increased the involvement of hydrophobic groups in binding (Sun et al., 2022). Differences in the intrinsic fluorescence spectra of dual proteins indicated changes in their tertiary structures, potentially affecting their solubility, stability, and interfacial properties.

3.1.5. UV spectra analysis

The UV absorption spectrum is sensitive to the tertiary structure of protein molecules, with UV absorbance typically correlates with protein conformational folding (Liu et al., 2009). As shown in Fig. 5B, SPI and TPI exhibited characteristic absorption at 200 nm and 197 nm, respectively, while the three dual proteins displayed similar absorption peaks at 200 nm and 205 nm. In the range of 205–240 nm, the UV spectra of T-SPC and T-SPCP demonstrated stronger absorption intensities than those of TPI and T-SPM, indicating enhanced interactions, potentially influenced by the surrounding environment of pH-altering molecules

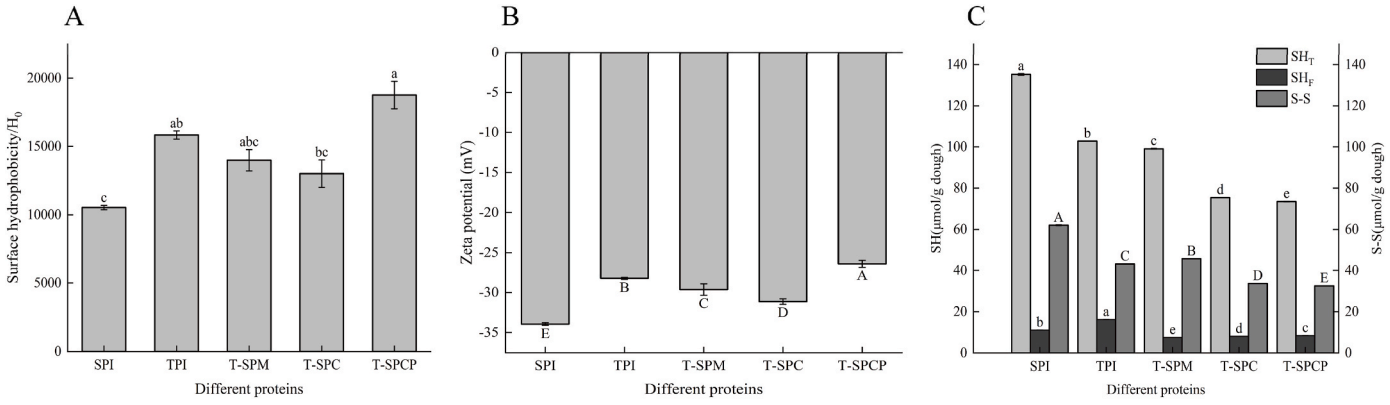

Fig. 4. Surface hydrophobicity (A), zeta potential (B), sulfhydryl and disulfide bond contents (C) of SPI, TPI and tilapia-soybean dual proteins. *Note:* Values with different letters in the graph indicate significant differences ($p < 0.05$).

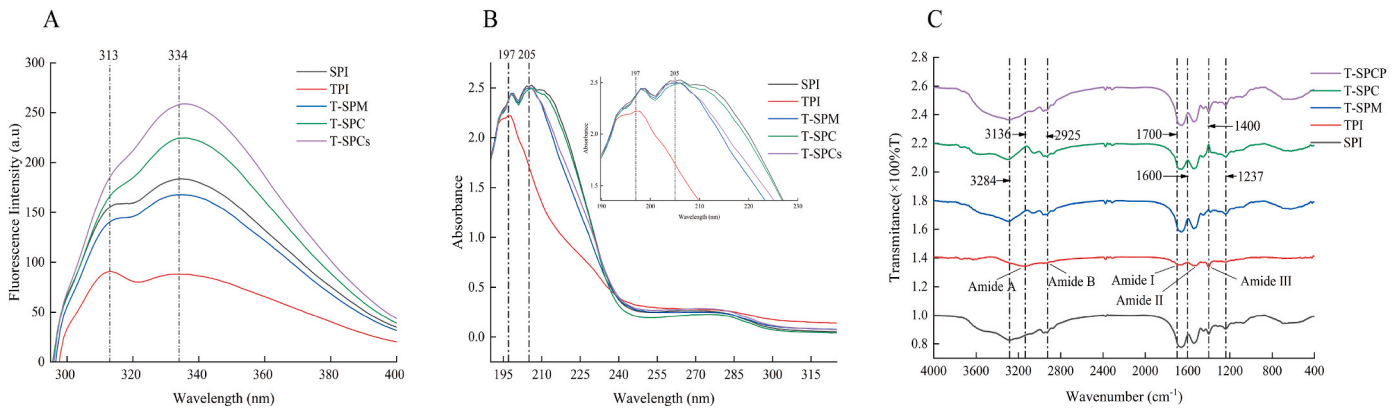

Fig. 5. Fluorescence spectra (A), UV spectra (B), and infrared spectra (C) of SPI, TPI and tilapia-soybean dual proteins.

such as hydrogen bonds and van der Waals forces (Tang and Shen, 2013). Previous studies have confirmed that under strongly alkaline conditions, peptide chains cross-link due to hydrogen bonding, hydrophobic interactions, and electrostatic interactions between protein molecules, leading to changes in protein aromatic amino acids (Yan et al., 2021). Therefore, the absorption strength of T-SPC and T-SPCP was greater than that of T-SPM. Additionally, the absorption peaks of T-SPC and T-SPCP exhibited slight redshifts compared to TPI, suggesting that the peptide chains of the dual proteins may have crosslinked during the pH shifting at 12.0. Combined with the results from fluorescence spectrum analysis, these findings further confirm that changes in the hydrophobic microenvironment of aromatic amino residues in protein molecules lead to the exposure of internal groups and alterations in protein structure, potentially affecting functional properties.

3.1.6. *Infrared spectra analysis*

FTIR is an effective method for monitoring changes in protein secondary structure. As shown in Fig. 5C, the broader peak area of dual protein samples indicates differences in molecular structure associated with changes in repulsion, electrostatic interactions, and hydrogen bonds. Additionally, the dual proteins exhibited a blueshift peak in the 1300-1200 cm^{-1} region (~1237 cm^{-1}), related to the stretching and bending of C-N and N-H bonds in the amide III band, indicating the presence of intramolecular or intermolecular interactions (Li et al., 2019).

Compared to SPI and TPI, the absorption intensity of T-SPC differed significantly, with T-SPC and T-SPCP exhibiting an obvious absorption peak at 3136 cm^{-1}, indicating structural changes in the dual proteins due to alterations in protein components and molecular interactions (Li et al., 2019). In the spectra of amide A (3500-3300 cm^{-1}, N-H stretching vibration), I (1700-1600 cm^{-1}, C=O stretching vibration), and II (1550-1530 cm^{-1}, N-H deformation vibration or C-N stretching motion) bands, the FTIR intensity of T-SPC, T-SPM, and T-SPCP was significantly stronger than that of TPI, with considerable shifts observed in the amide B (1780-1680 cm-1, C=O stretching vibration and N-H bending vibration) and amide III (1300-1260 cm^{-1}, C-N stretching vibration, and N-H plane bending vibration) bands. These results further indicate that T-SPC has stronger intramolecular and intermolecular hydrogen bond interactions than TPI. Therefore, the FTIR spectral results revealed the coexistence and interaction of TPI and SPI structures in T-SPM, T-SPC, and T-SPCP. Combined with the SDS-PAGE analysis results, this confirms the coexistence of TPI and SPI components in the three dual proteins. Additionally, T-SPC exhibited different absorption intensities compared to T-SPM and T-SPCP, suggesting it may possess a unique structure. Consequently, the dual proteins differ in structure, with T-SPC being exceptional, which may lead to distinct properties.

3.1.7. *Circular dichroism spectra and secondary structure content*

To further investigate the structural variability among the five kinds of proteins, the secondary structure contents were calculated from the far-UV CD spectra using the CONTIN/LL program in CDNN software. The far-ultraviolet CD spectra (Fig. 6A) revealed wide negative bands in the 200–240 nm range for the dual proteins of T-SPM, T-SPC, and T-SPCP, which prove that there are multiple secondary structures in these dual proteins. In the CD spectra, the absorption peaks of α-helix structures exhibited positive bands around 192 nm and negative bands at 208 nm and 222 nm. Compared to TPI and SPI, the positions and intensities of the peaks in the CD spectra of the dual proteins were changed significantly, indicating that complexation notably altered the secondary structures of the proteins (Yan et al., 2022).

The α-helix structure content increased in T-SPC and T-SPCP, while the β-folded structure decreased, suggesting a tendency for the protein structure to transition to a more ordered form. The increase in α-helix may result from the solubilization of more myofibrillar proteins following the addition of SPI and pH adjustment. The change in sodium ion concentration will affect the ionic strength of the solution and other properties, thus changing the microenvironment of the protein. Such microenvironmental changes may affect non-covalent interactions such as hydrogen bonding and van der Waals forces within proteins. For example, in an environment of high ionic strength, some hydrogen bonds within the protein molecule may be destroyed due to the competitive effect of ions on hydrogen bonds, and then the secondary structure of the protein such as α-helix, β-folding, etc., and will eventually affect the overall structure and functional properties of the protein (Wei et al., 2019). The pH-shifting treatment exposed more buried protein molecular residues to water molecules, facilitating the formation of new hydrogen bonds crucial for maintaining the structural stability of the α-helix (Liu et al., 2008). A decrease in β-folded structures can be attributed to reductions in SH_T and H_0 (Fig. 4). Generally, changes in SH_T and H_0 are closely related to the secondary structural information of myofibrillar proteins (Du et al., 2018). Among the dual proteins, T-SPM exhibited the lowest α-helix structure content and the highest β-folding and irregular curl content. This indicates that while the dual protein structure tends to unfold, the simple physical mixing of T-SPM leads to a disordered structure, which is unfavorable for protein stability. Furthermore, the increase in α-helix structure may relate to the addition of SPI disrupting the electrostatic interactions of the protein molecules (Fig. 4A), consistent with the results regarding average potential. The increase in α-helix is also associated with enhanced protein solubility, with T-SPC and T-SPCP showing the most significant changes.

3.1.8. *SEM analysis*

In Fig. 7, SPI displayed a dense spherical composition with regular edges, while TPI exhibited a porous, lamellar, and loose microstructure with rough and irregular edges. At the same magnification, the volume

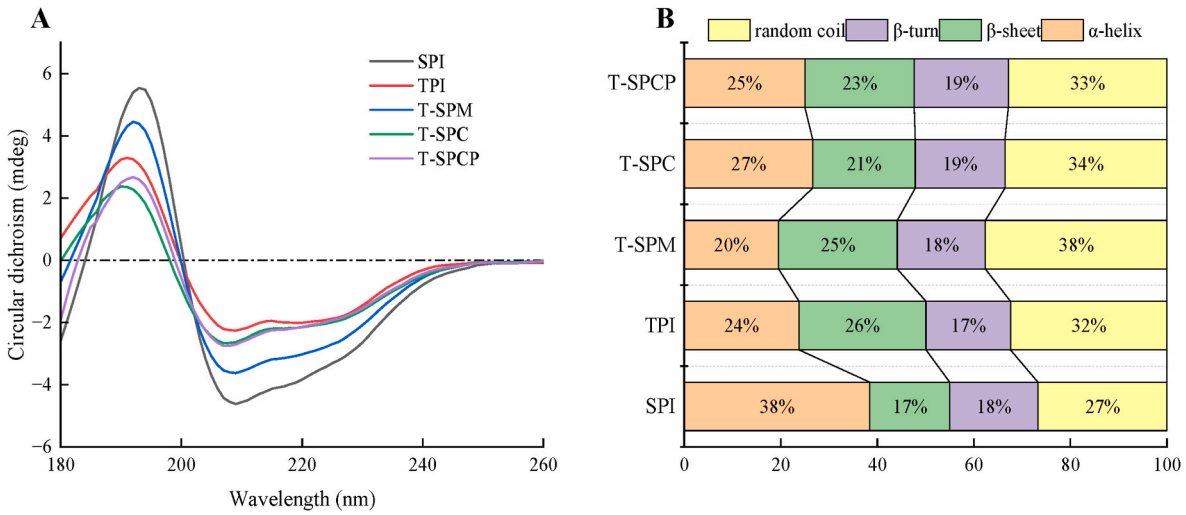

Fig. 6. Circular dichroism (A) and protein secondary structure content (B) of SPI, TPI and tilapia-soybean dual proteins.

structure of SPI was smaller than that of TPI. Additionally, the shape and volume of the protein samples changed following the preparation of dual proteins using different pH-regulated methods. In T-SPM, spherical SPI was bound to larger TPI, with SPI primarily adhering to the surface of TPI and a small amount bound to its inner part, forming an irregular shape. The structure of the flake protein block was dense and compact, lacking micro-pores. In T-SPC, SPI adhered mainly to the surface of TPI, with some SPI bound to the internal surface, resulting in an irregular shape. T-SPCP exhibited more dense microporous structures than T-SPC. A further co-precipitation at pH 4.5 in the preparing T-SPCP caused the precipitation and polymerization of proteins due to anti-solvent action (Sui et al., 2017), resulting in large-complex protein particles exposing hydrophobic regions and forming irregular polymers due to a loose internal structure. So T-SPCP may have lower solubility and higher thermal stability. Overall, the dual proteins of T-SPC and T-SPCP exhibited a more complex cross-linked three-dimensional structure and had a smaller volume than the fish proteins alone at the same magnification.

3.2. Functional properties characterization

3.2.1. Solubility analysis

Functional properties of protein are closely related to solubility, which determines its potential application in food (Wang et al., 2018). As shown in Fig. 8A, SPI exhibited the highest solubility, while TPI had the lowest ($p < 0.05$). The solubility of the dual proteins fell between those of SPI and TPI ($p < 0.05$). Compared to TPI, the solubility of T-SPM, T-SPC, and T-SPCP increased by 64.6 %, 67.4 %, and 54.0 %, respectively. Protein solubility is also linked to surface hydrophobicity and charge potential. As shown in Fig. 8, the solubility of T-SPC was higher than that of T-SPM and T-SPCP, likely due to a pH adjustment of 12.0, which increased the exposure of charged groups on the protein surface. This enhanced intermolecular repulsion and electronegativity, contributing to protein stability and solubility (Chelh et al., 2006). Thus, the solubility of T-SPC is significantly greater than that of TPI and the other dual proteins. The reduced solubility of T-SPCP may result from enhanced protein interactions due to increased hydrophobicity.

3.2.2. EAI and ESI analysis

Emulsifying capacity, which reflects the ability of proteins to absorb at the oil-water interface, is typically evaluated using EAI and ESI (Moure et al., 2006). As shown in Fig. 8B, the EAI of SPI was 27.18 m^2/g, while the EAI of TPI was lower at 10.80 m^2/g. The EAI values of the three dual proteins were significantly higher than that of TPI ($p < 0.05$). The ESI value of T-SPCP was significantly higher than those of T-SPC and T-SPM ($p < 0.05$). In the emulsion system, the emulsifying performance may not solely be attributed to the complexes themselves, as the physical mixture of SPI and TPI did not exhibit significantly improved EAI and ESI values (Fig. 8B). T-SPC has a poor ESI but a good EAI. This discrepancy cannot be explained solely by the structural characteristics of T-SPC, as pH variation also influences the structure of T-SPCP. Interestingly, T-SPCP assembled by pH-regulation from 12.0 to 4.5 exhibited a higher ESI. This indicated that EAI and ESI are not always correlated (Barac et al., 2010). The structural characteristics of T-SPCP, particularly the modification of surface groups (Fig. 4A), further supported its enhanced ESI functionality. The significant reduction in ESI for T-SPC may be related to differences in the degree of structural unfolding caused by pH adjustment, which differed from the refolding and interactions of the protein when neutralized to pH 7.0 after acidic pH adjustment. Protein molecules that unfold at pH 12.0 may refold upon further adjustment to pH 4.5 or 7.0. However, due to the exposure of internal groups and the stretching of the overall structure, different protein molecules within the dual protein interact with each other (Sui et al., 2017). In the emulsions prepared under these conditions, the interactions between protein molecules increase, slowing down droplet aggregation, flocculation, and other instabilities caused by gravity or Brownian motion (Bos, 2001). Moreover, within a certain range, increased surface hydrophobicity enhances the adsorption of molecules at the oil-water interface (Fig. 4A). These results are align with Thompson's (Thompson, 1978) study, confirming that T-SPCP and T-SPC exhibited higher EAI and ESI values compared to T-SPM and TPI. The improvement in the emulsifying performance of dual proteins corresponded to the changes in solubility (Fig. 8A), indicating that the emulsification of the composite dual protein was enhanced compared to that of TPI.

3.2.3. FC and FS analysis

FC relates to the ability of protein to form liquid or air dispersion and is strongly associated with the two-phase interface. FS represents the percentage of protein remaining in the initial foam volume over time; proteins with good FS also exhibit better hydration (Cao et al., 2009). As shown in Fig. 8C, compared to SPI (32.5 %) and TPI (18.75 %), the foamability of the dual proteins was significantly improved ($p < 0.05$). Among them, T-SPC prepared by pH-regulated complexation exhibited the greatest FC and FS, followed by T-SPCP and T-SPM. The foaming properties of proteins are influenced by various factors, including solubility, protein conformation, molecular interactions, and aggregate formation (Yang et al., 2021). As shown in Fig. 6B, T-SPC exhibited the highest α-helix content among the dual proteins, which positively

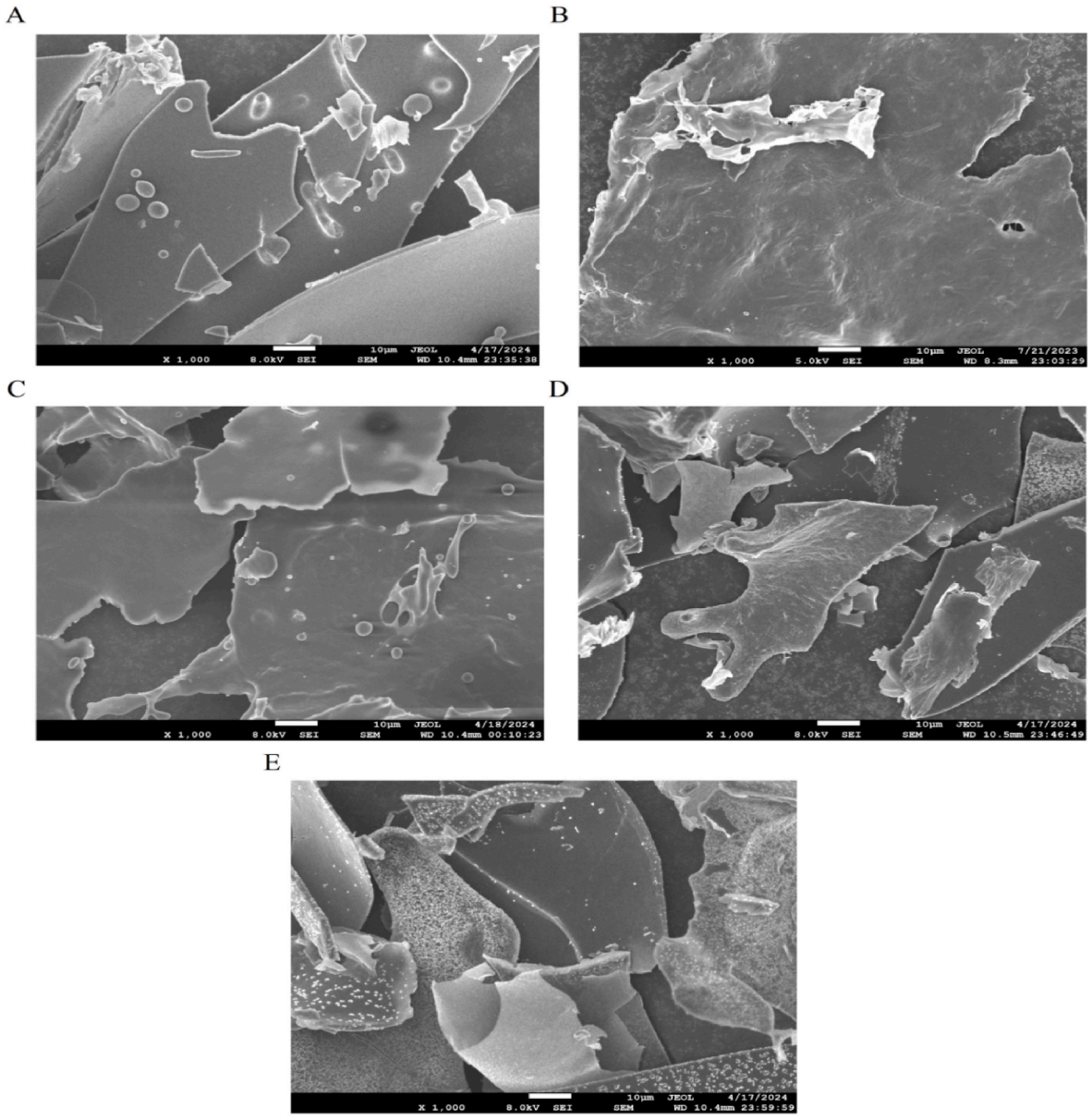

Fig. 7. Scanning electron micrographs of SPI (A), TPI (B), T-SPM (C), T-SPC (D), and T-SPCP (E).

correlated with the molecular flexibility and facilitated protein dispersion at the air-water interface. Foaming properties are also associated with H_0 (Yang et al., 2021), and a higher H_0 means greater exposure to hydrophobic clusters, enhancing interactions between the protein molecules and the gas phase. The pH adjustment to 12.0 caused molecular unfolding, thereby increasing the exposure of hydrophobic regions (Nazari et al., 2018), whereas the co-precipitation at pH 4.5 resulted in extensive aggregation of protein molecules. Consequently, T-SPCP molecules characterized by high surface hydrophobicity (Fig. 4) are significantly limited in their ability to diffuse to the air-water interface and form an interfacial film (Pezeshk et al., 2021), resulting in lower foamability compared to T-SPC.

3.2.4. *Thermal stability analysis*

In DSC curves, exothermic peaks are represented as upward deviations, whereas endothermic peaks are depicted as downward deviations. These peak changes provide insights into the phase transition phenomena during heating or cooling, contributing to a comprehensive understanding of how different preparation methods influence the thermal stability of composite proteins. As shown in Fig. 8D, the thermal denaturation temperatures (T_d) of SPI and TPI were 71 °C and 65.5 °C, respectively. The T_d values of T-SPM, T-SPC, and T-SPCP were 67 °C, 67.5 °C, and 70.6 °C, respectively, higher than that of TPI but lower than that of SPI. The temperature variations of major peaks indicate interactions between protein components, which influence their thermal behavior (Ricci et al., 2018). Wright et al. (Wright and Wilding, 1984) observed that different sub-fragments of myofibrillar proteins exhibit varying behaviors in response to environmental changes, indicating that myofibrillar proteins undergo one or more transitions, with pH playing a significant role in the conformational stability of these fragments. These factors result in variations in peak denaturation temperatures during heating (Nawrocka et al., 2017). Consequently, the thermal denaturation temperature of T-SPCP was higher than those of T-SPM and T-SPC, likely due to the cross-linking aggregation of complex proteins, leading to the formation of larger aggregate particles during co-precipitation at pH 4.5.

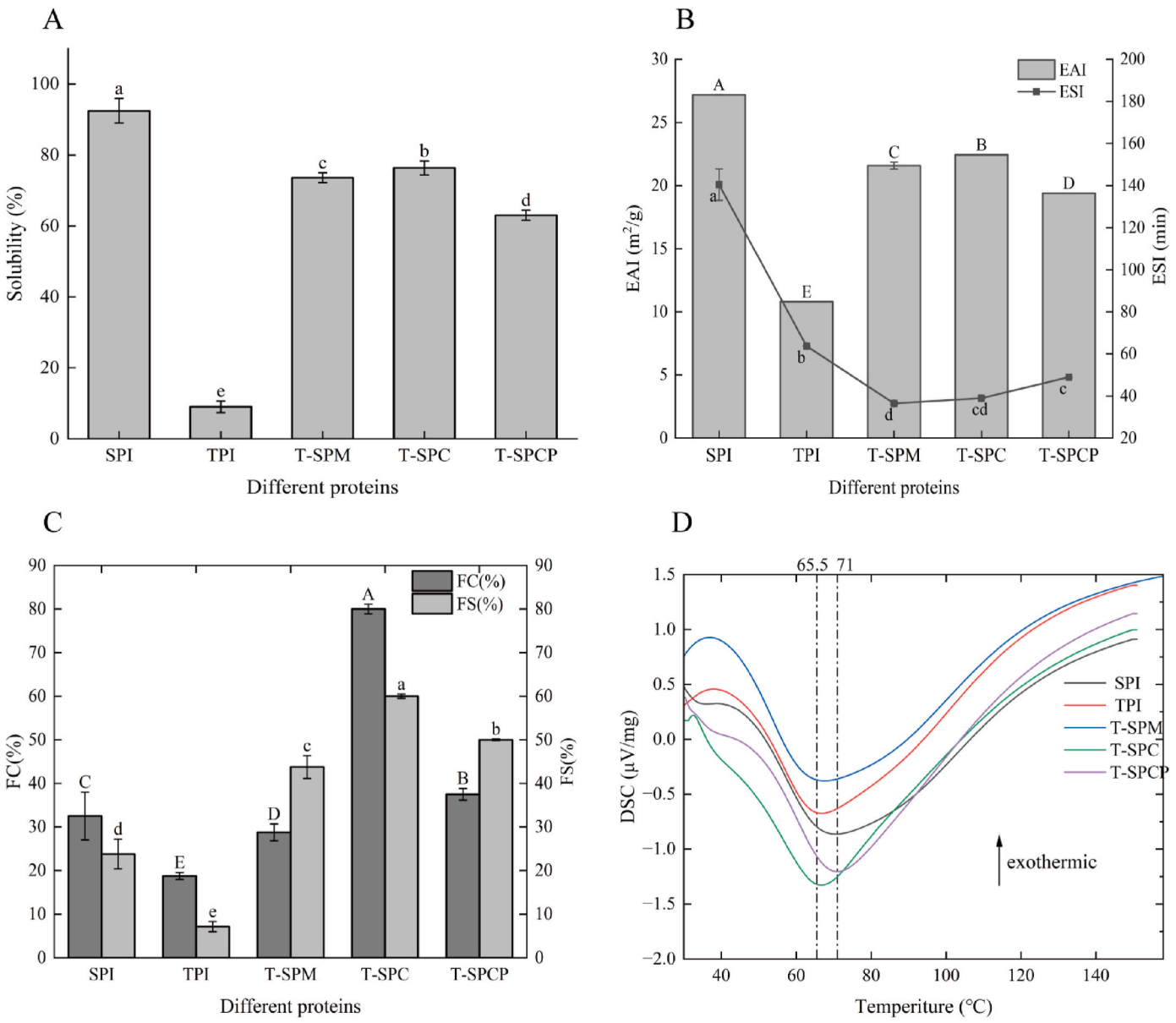

Fig. 8. Solubility (A), emulsifying activity and emulsifying stability (B), foaming capacity and foam stability (C), and DSC curves (D) of SPI, TPI and tilapia-soybean dual proteins.

4. Conclusions

TPI and SPI primarily co-assemble into tilapia-soybean dual proteins through non-covalent interactions and disulfide bonds. The dual proteins prepared by physical mixing and pH-regulated complexation or co-precipitation exhibited different characteristics. Compared to T-SPM, T-SPC and T-SPCP, both prepared by pH-regulated assembly have enhanced functional characteristics. In particular, T-SPC differed significantly, and it has a more hydrophilic structure with superior water solubility, emulsifying ability, and foaming capacity. T-SPCP displayed better thermal stability with a more aggregated structure and larger particles caused by pH adjustment to 4.5 during the co-precipitation. Therefore, T-SPC assembled by pH-regulation from 12.0 to 7.0 is suitable for widespread use as nutritional supplements or bioactive compound delivery systems. T-SPCP assembled by pH-regulation from 12.0 to 4.5 supports their incorporation into formulated proteins. In conclusion, pH-regulated assembly is an effective way to prepare dual proteins from different sources; it can effectively regulate the functional properties and application range of dual proteins. This study will provide ideas and references for rationally selecting protein recombination technologies to improve the functional properties of aquatic proteins. It also offers a theoretical basis for applying functional aquatic proteins in protein emulsifiers and functional protein powders. However, the current research has not conducted a comparative analysis of the protein composition and nutritional characteristics of dual-protein systems prepared by different compounding methods. Therefore, future research should use proteomic techniques to compare the differences in the protein composition of dual-protein systems prepared by different compounding methods, and further analyze their nutritional characteristics.

CRediT authorship contribution statement

Xinyi Qin: Carried out experiments, wrote initial manuscript and revised the first draft in response to the comments of others. **Pengzhi Hong:** Put forward important suggestions for revision of the first draft. **Liangyu Zhao:** Put forward important suggestions for revision of the first draft. **Mengya Xie:** Put forward important suggestions for revision

of the first draft. **Chunxia Zhou:** Put forward suggestions for revision of the first draft, and proofread of the revised manuscripts, including grammar and content. **Qingguan Liu:** Oversight and leadership responsibility for the research activity planning and execution.

Declaration of competing interest

The authors confirm that they have no conflict of interest to declare for this publication.

Acknowledgements

This work was supported by the Guangdong Modern Agricultural Industrial Technology System Innovation Team Building Project (2023KJ150), Zhanjiang Science and Technology Program Project (2022A05037), and Scientific research start-up funds of Guangdong Ocean University (060302042317).

Data availability

Data will be made available on request.

References

Agyare, K.K., Addo, K., Xiong, Y.L., 2009. Emulsifying and foaming properties of transglutaminase-treated wheat gluten hydrolysate as influenced by pH, temperature and salt. Food Hydrocoll. 23, 72–81. https://doi.org/10.1016/j.foodhyd.2007.11.012.

Ali Mekouar 15, M., 2019. Food and agriculture organization of the united nations (FAO). Yearbook of International Environmental Law 28, 506–520. https://doi.org/10.1093/yiel/yvy073.

Alves, A.C., Tavares, G.M., 2019. Mixing animal and plant proteins: is this a way to improve protein techno-functionalities? Food Hydrocoll. 97, 105171. https://doi.org/10.1016/j.foodhyd.2019.06.016, 105171-105171.105110.

Barac, M., Cabrilo, S., Pesic, M., Stanojevic, S., Zilic, S., Macej, O., Ristic, N., 2010. Profile and functional properties of seed proteins from six pea (*Pisum sativum*) genotypes. Int. J. Mol. Sci. 11, 4973–4990. https://doi.org/10.3390/ijms11124973.

Beveridge, T., Toma, S.J., Nakai, S., 1974. Determination of SH- and -SS- groups in some food proteins using Ellman's reagent. J. Food Sci. 39, 49–51. https://doi.org/10.1111/j.1365-2621.1974.tb00984.x.

Bos, T.v.V. Martin A., 2001. Interfacial rheological properties of adsorbed protein layers and surfactants a review. Adv. Colloid Interface Sci. 91, 437–471. https://doi.org/10.1016/s0001-8686(00)00077-4.

Britten, M., Giroux, H., Gaudin, V., 1994. Effect of pH during heat processing of partially hydrolyzed whey protein. Dairy Sci 77, 676–684. https://doi.org/10.3168/jds.s0022-0302(94)76999-x.

Cao, X., Wen, H., Li, C., Gu, Z., 2009. Differences in functional properties and biochemical characteristics of congenetic rice proteins. J. Cereal. Sci. 50, 184–189. https://doi.org/10.1016/j.jcs.2009.04.009.

Chelh, I., Gatellier, P., Santé-Lhoutellier, V., 2006. Technical note: a simplified procedure for myofibril hydrophobicity determination. Meat Sci. 74, 681–683. https://doi.org/10.1016/j.meatsci.2006.05.019.

Cheng, Y., Ye, A., Singh, H., 2024. Characterizations of emulsion gel formed with the mixture of whey and soy protein and its protein digestion under in vitro gastric conditions. Curr. Res. Food Sci. 8. https://doi.org/10.1016/j.crfs.2023.100674.

Du, X.J., Sun, Y.Y., Pan, D.D., Wang, Y., Ou, C.R., Cao, J.X., 2018. The effect of structural change on the digestibility of sarcoplasmic proteins in Nanjing dry-cured duck during processing. Poult. Sci. 97, 4450–4457. https://doi.org/10.3382/ps/pey316.

Guo Huang, G.L., Xu, Zejian, Jiang, Lianzhou, Zhang, Yan, Sui, Xiaonan, 2023. Stability, rheological behavior and microstructure of Pickering emulsions co-stabilized by soy protein and carboxymethyl chitosan. Food Hydrocoll. 142. https://doi.org/10.1016/j.foodhyd.2023.108773.

Han, Z., Cai, M.j., Cheng, J.H., Sun, D.W., 2019. Effects of microwave and water bath heating on the interactions between myofibrillar protein from beef and ketone flavour compounds. Int. J. Food Sci. Technol. 54, 1787–1793. https://doi.org/10.1111/ijfs.14079.

Jafarzadeh, S., Qazanfarzadeh, Z., Majzoobi, M., Sheiband, S., Oladzadabbasabad, N., Esmaeili, Y., Barrow, C.J., Timms, W., 2024. Alternative proteins; A path to sustainable diets and environment. Curr. Res. Food Sci. 9. https://doi.org/10.1016/j.crfs.2024.100921.

Jiang, J., Chen, J., Xiong, Y.L., 2009. Structural and emulsifying properties of soy protein isolate subjected to acid and alkaline pH-shifting processes. J. Agric. Food Chem. 57, 7576–7583. https://doi.org/10.1021/jf901585n.

Jianhua Liu, C.F., Xu, Xia, Su, Qi, Zhao, Peicheng, Ding, Yuting, 2019. Structural changes of silver carp myosin glycated with konjac oligo-glucomannan: effects of deacetylation. Food Hydrocoll. 91, 275–282. https://doi.org/10.1016/j.foodhyd.2019.01.038.

Kheto, A., Sehrawat, R., Gul, K., Kumar, L., 2024. Effect of extraction pH on amino acids, nutritional, in-vitro protein digestibility, intermolecular interactions, and functional properties of guar germ proteins. Food Chem. 444. https://doi.org/10.1016/j.foodchem.2024.138628.

Kristensen, H.T., Christensen, M., Hansen, M.S., Hammershøj, M., Dalsgaard, T.K., 2022. Mechanisms behind protein-protein interactions in a β-lg-legumin co-precipitate. Food Chem. 373. https://doi.org/10.1016/j.foodchem.2021.131509.

Li, R., Wang, X., Liu, J., Cui, Q., Wang, X., Chen, S., Jiang, L., 2019. Relationship between molecular flexibility and emulsifying properties of soy protein isolate-glucose conjugates. J. Agric. Food Chem. 67, 4089–4097. https://doi.org/10.1021/acs.jafc.8b06713.

Li, X., Hong, P., Xie, M., Wang, Y., Liu, Q., Zhou, C., 2024. Formation of hydrophilic co-assemblies with improved functional properties between tilapia protein isolate and sodium caseinate. Food Hydrocoll. 153. https://doi.org/10.1016/j.foodhyd.2024.110016.

Lin, D., Lu, W., Kelly, A.L., Zhang, L., Zheng, B., Miao, S., 2017. Interactions of vegetable proteins with other polymers: structure-function relationships and applications in the food industry. Trends Food Sci. Technol. 68, 130–144. https://doi.org/10.1016/j.tifs.2017.08.006.

Liu, G., Xiong, Y.L., 2000. Electrophoretic pattern, thermal denaturation, and in vitro digestibility of oxidized myosin. J. Agric. Food Chem. 624–630. https://doi.org/10.1021/jf990520h.

Liu, R., Zhao, S.-m., Xiong, S.-b., Xie, B.-j., Qin, L.-h., 2008. Role of secondary structures in the gelation of porcine myosin at different pH values. Meat Sci. 80, 632–639. https://doi.org/10.1016/j.meatsci.2008.02.014.

Liu, P.-F., Avramova, L.V., Park, C., 2009. Revisiting absorbance at 230nm as a protein unfolding probe. Anal. Biochem. 389, 165–170. https://doi.org/10.1016/j.ab.2009.03.028.

Liu, Y., Zhao, G., Zhao, M., Ren, J., Yang, B., 2012. Improvement of functional properties of peanut protein isolate by conjugation with dextran through Maillard reaction. Food Chem. 131, 901–906. https://doi.org/10.1016/j.foodchem.2011.09.074.

Liu, Q., Tan, L., Hong, P., Liu, H., Zhou, C., 2024. Tilapia-soybean protein co-precipitates: focus on physicochemical properties, nutritional quality, and proteomics profile. Food Chem. X 21. https://doi.org/10.1016/j.fochx.2024.101179.

Mohan, M., Ramachandran, D., Sankar, T.V., 2006. Functional properties of Rohu (*Labeo rohita*) proteins during iced storage. Food Res. Int. 39, 847–854. https://doi.org/10.1016/j.foodres.2006.04.003.

Moure, A., Sineiro, J., Domínguez, H., Parajó, J.C., 2006. Functionality of oilseed protein products: a review. Food Res. Int. 39, 945–963. https://doi.org/10.1016/j.foodres.2006.07.002.

National date. https://data.stats.gov.cn, 2024. URL (accessed 20 Auguest 2024).

Nawrocka, A., Szymańska-Chargot, M., Miś, A., Wilczewska, A.Z., Markiewicz, K.H., 2017. Effect of dietary fibre polysaccharides on structure and thermal properties of gluten proteins – a study on gluten dough with application of FT-Raman spectroscopy, TGA and DSC. Food Hydrocoll. 69, 410–421. https://doi.org/10.1016/j.foodhyd.2017.03.012.

Nazari, B., Mohammadifar, M.A., Shojaee-Aliabadi, S., Feizollahi, E., Mirmoghtadaie, L., 2018. Effect of ultrasound treatments on functional properties and structure of millet protein concentrate. Ultrason. Sonochem. 41, 382–388. https://doi.org/10.1016/j.ultsonch.2017.10.002.

Pezeshk, S., Rezaei, M., Hosseini, H., Abdollahi, M., 2021. Impact of pH-shift processing combined with ultrasonication on structural and functional properties of proteins isolated from rainbow trout by-products. Food Hydrocoll. 118. https://doi.org/10.1016/j.foodhyd.2021.106768.

Pramono, H., Irawan, N.T., Firdaus, M.R.A., 2019. Characteristics of the fish protein isolate recovered from Sardine by-products using the Isoelectric Solubilization-Precipitation method. IOP Conf. Ser. Earth Environ. Sci. 236. https://doi.org/10.1088/1755-1315/236/1/012112.

Ricci, L., Umilta, E., Righetti, M.C., Messina, T., Zurlini, C., Montanari, A., Bronco, S., Bertoldo, M., 2018. On the thermal behavior of protein isolated from different legumes investigated by DSC and TGA. J. Sci. Food Agric. 98, 5368–5377. https://doi.org/10.1002/jsfa.9078.

Shaheen, N., Islam, S., Munmun, S., Mohiduzzaman, M., Longvah, T., 2016. Amino acid profiles and digestible indispensable amino acid scores of proteins from the prioritized key foods in Bangladesh. Food Chem. 213, 83–89. https://doi.org/10.1016/j.foodchem.2016.06.057.

Song, X., Zhou, C., Fu, F., Chen, Z., Wu, Q., 2013. Effect of high-pressure homogenization on particle size and film properties of soy protein isolate. Ind. Crop. Prod. 43, 538–544. https://doi.org/10.1016/j.indcrop.2012.08.005.

Sui, X., Bi, S., Qi, B., Wang, Z., Zhang, M., Li, Y., Jiang, L., 2017. Impact of ultrasonic treatment on an emulsion system stabilized with soybean protein isolate and lecithin: its emulsifying property and emulsion stability. Food Hydrocoll. 63, 727–734. https://doi.org/10.1016/j.foodhyd.2016.10.024.

Sun, Y., Chen, H., Chen, W., Zhong, Q., shen, Y., Zhang, M., 2022. Effect of ultrasound on pH-shift to improve thermal stability of coconut milk by modifying physicochemical properties of coconut milk protein. Lwt 167. https://doi.org/10.1016/j.lwt.2022.113861.

Tang, C.-H., Shen, L., 2013. Role of conformational flexibility in the emulsifying properties of bovine serum albumin. J. Agric. Food Chem. 61, 3097–3110. https://doi.org/10.1021/jf305471k.

Thompson, L.U., 1978. Coprecipitation of cheese whey with soybean and cottonseed. Food Technologists 43, 790–792. https://doi.org/10.1111/j.1365-2621.1978.tb02420.x.

Tian, H., Guo, G., Fu, X., Yao, Y., Yuan, L., Xiang, A., 2018. Fabrication, properties and applications of soy-protein-based materials: a review. Int. J. Biol. Macromol. 120, 475–490. https://doi.org/10.1016/j.ijbiomac.2018.08.110.

Tian, T., Ren, K., Tong, X., Peng, X., Lian, Z., Lyu, B., Du, M., Wang, H., Jiang, L., 2022. Co-precipitates proteins prepared by soy and wheat: structural characterisation and

functional properties. Int. J. Biol. Macromol. 212, 536–546. https://doi.org/10.1016/j.ijbiomac.2022.05.149.
Wang, L., Zhang, M., Fang, Z., Bhandari, B., 2016. Gelation properties of myofibrillar protein under malondialdehyde-induced oxidative stress. J. Sci. Food Agric. 97, 50–57. https://doi.org/10.1002/jsfa.7680.
Wang, T., Xu, P., Chen, Z., Wang, R., 2018. Mechanism of structural interplay between rice proteins and soy protein isolates to design novel protein hydrocolloids. Food Hydrocoll. 84, 361–367. https://doi.org/10.1016/j.foodhyd.2018.06.024.
Wang, B., Kong, B., Li, F., Liu, Q., Zhang, H., Xia, X., 2020a. Changes in the thermal stability and structure of protein from porcine longissimus dorsi induced by different thawing methods. Food Chem. 316. https://doi.org/10.1016/j.foodchem.2020.126375.
Wang, R., Li, L., Feng, W., Wang, T., 2020b. Fabrication of hydrophilic composites by bridging the secondary structures between rice proteins and pea proteins toward enhanced nutritional properties. Food Funct. 11, 7446–7455. https://doi.org/10.1039/d0fo01182g.
Wang, R., Wang, T., Feng, W., Wang, Q., Wang, T., 2021. Rice proteins and cod proteins forming shared microstructures with enhanced functional and nutritional properties. Food Chem. 354. https://doi.org/10.1016/j.foodchem.2021.129520.
Wang, R., Wang, L.-H., Wen, Q.-H., He, F., Xu, F.-Y., Chen, B.-R., Zeng, X.-A., 2023. Combination of pulsed electric field and pH shifting improves the solubility, emulsifying, foaming of commercial soy protein isolate. Food Hydrocoll. 134. https://doi.org/10.1016/j.foodhyd.2022.108049.
Wei, L., Cao, L., Xiong, S., You, J., Hu, Y., Liu, R., 2019. Effects of pH on self-assembly of silver carp myosin at low temperature. Food Biosci. 30. https://doi.org/10.1016/j.fbio.2019.100420.
Wright, D.J., Wilding, P., 1984. Differential scanning calorimetric study of muscle and its proteins myosin and its subfragments. Food Agric 35, 357–372. https://doi.org/10.1002/jsfa.2740350317.
Yan, S., Xu, J., Zhang, S., Li, Y., 2021. Effects of flexibility and surface hydrophobicity on emulsifying properties: ultrasound-treated soybean protein isolate. Lwt 142. https://doi.org/10.1016/j.lwt.2021.110881.
Yan, S., Yao, Y., Xie, X., Zhang, S., Huang, Y., Zhu, H., Li, Y., Qi, B., 2022. Comparison of the physical stabilities and oxidation of lipids and proteins in natural and polyphenol-modified soybean protein isolate-stabilized emulsions. Food Res. Int. 162, 112066. https://doi.org/10.1016/j.foodres.2022.112066.
Yang, W., Tu, Z., Li, Q., Kaltashov, I.A., McClements, D.J., 2021. Utilization of sonication-glycation to improve the functional properties of ovalbumin: a high-resolution mass spectrometry study. Food Hydrocoll. 119. https://doi.org/10.1016/j.foodhyd.2021.106822.
Yin Zonglun Wang, T.S., 2007. The ‘double protein Project’ and the strength of the Chinese nation - realising premier wen’s ‘dream’ with the ‘double protein Project’ revitalisation plan. China Food Journal 1–5. https://doi.org/10.16429/j.1009-7848.2007.01.001.
Zhao, R., Fu, W., Li, D., Dong, C., Bao, Z., Wang, C., 2024. Structure and functionality of whey protein, pea protein, and mixed whey and pea proteins treated by pH shift or high-intensity ultrasound. J. Dairy Sci. 107, 726–741. https://doi.org/10.3168/jds.2023-23742.